ANALYTICAL SCIENCES NOVEMBER 2016, VOL. 32

Morphological and Mechanical Properties of Osteosarcoma Microenvironment Cells Explored by Atomic Force Microscopy

Xinlong WANG,*, Yingjun YANG,*,** Xiaohong HU,*,*** Naoki KAWAZOE,* Yingnan YANG,*** and Guoping CHEN*,**†**

**International Center for Materials Nanoarchitectonics, National Institute for Materials Science, 1-1 Namiki, Tsukuba, Ibaraki 305-0044, Japan*
***Department of Materials Science and Engineering, Graduate School of Pure and Applied Sciences, University of Tsukuba, 1-1-1 Tennodai, Tsukuba, Ibaraki 305-8571, Japan*
****Graduate School of Life and Environmental Science, University of Tsukuba, 1-1-1 Tennodai, Tsukuba, Ibaraki 305-8571, Japan*

Cell mechanical properties that depend on cytoskeleton architecture are critical to the mechanotransduction process, and have great potential for cancer diagnosis and therapy. In this study, the morphological and mechanical properties of typical osteosarcoma microenvironment cells, including mesenchymal stem cells (MSC), normal human osteoblast cells (NHOst) and osteosarcoma cells (MG-63), were compared using atomic force microscopy (AFM). The MG-63 cells were smaller and thicker than the MSC and NHOst cells. The membrane roughness of MG-63 cells was higher than that of MSC and NHOst cells. The MG-63 cells had lower stiffness than their normal counterparts due to their reduced organization of the cytoskeleton structure. The cell stiffness influenced the mechanotransduction. The MG-63 cells had a lower percentage of nuclear YAP/TAZ compared with the MSC and NHOst cells. The F-actin assembly was disrupted by the cytochalasin D (cyto D) treatment used to investigate its influence on mechanotransduction. Disruption of the cytoskeleton leaded to a decrease of the cell stiffness, and reduced the nuclear YAP/TAZ percentage, indicating its inhibition in the cell mechanotransduction process. This study would shed light on the development of a novel cancer diagnosis strategy and would contribute to reveal the relationship between the cytoskeleton structure and the cell mechanical properties.

Keywords AFM, cell stiffness, osteosarcoma environment cells, mechanotransduction, YAP/TAZ

(Received June 30, 2016; Accepted August 1, 2016; Published November 10, 2016)

Introduction

The cell mechanical properties are highly related to the mechanotransduction process, and play crucial roles in regulating cell behaviors. For instance, when mesenchymal stem cells (MSC) have high cytoskeleton tension, the activated Yes-associated proteins (YAP) and transcriptional coactivator with the PDZ-binding motif (TAZ) are accumulated in nuclei, indicating that the mechanical force is transmitted into cell nuclei, and that the cells undergo the osteogenic differentiation. On the other hand, YAP/TAZ is mainly distributed in cytoplasm when MSC cells have low cytoskeleton tension.[1] Some other types of stem cells, such as epidermal stem cells[2] and embryonic stem cells,[3,4] differentiate into various populations when they have different mechanical properties. Recently, the different mechanical properties between cancer cells and their normal counterparts are supposed to provide a new biomarker for the diagnosis and treatment of cancers.[5] Cancer transformation and progression are usually accompanied with mechanical property changes.[6] Also, many types of cancer and malignant cells have been reported to be softer than their normal and benign counterparts because of reduced organization of the cytoskeleton structure, which can increase their ability to penetrate tissues and the extracellular matrix.[7,8] Therefore, studies on the biomechanics of cells that are in the same microenvironment or lineage are greatly useful to both tissue engineering and cancer diagnosis and therapy.

Various techniques have been developed to evaluate the cell mechanical state, including the micropipette aspiration (MA),[9] optical stretcher (OP),[10] magnetic twisting cytometry (MTC),[11] traction force microscopy (TFM)[12] and atomic force microscopy (AFM).[13,14] MA and OP are most commonly used to acquire the rheological properties of suspended cells. Also, MTC and TFM can be used to measure the cytoskeletal contractive force based on the rotation of magnetic microbeads attached to the cell membrane (MTC) or the displacement of microbeads embedded in the cell culture substrate (TFM). AFM has the highest spatial resolution and the largest force range compared with the other techniques.[15] AFM indents the cell surface with a probe that is attached to a flexible cantilever. The indentation force is proportional to the deflection of the cantilever. According to the obtained force-indentation curve, the modulus of adherent cells

† To whom correspondence should be addressed.
E-mail: Guoping.CHEN@nims.go.jp

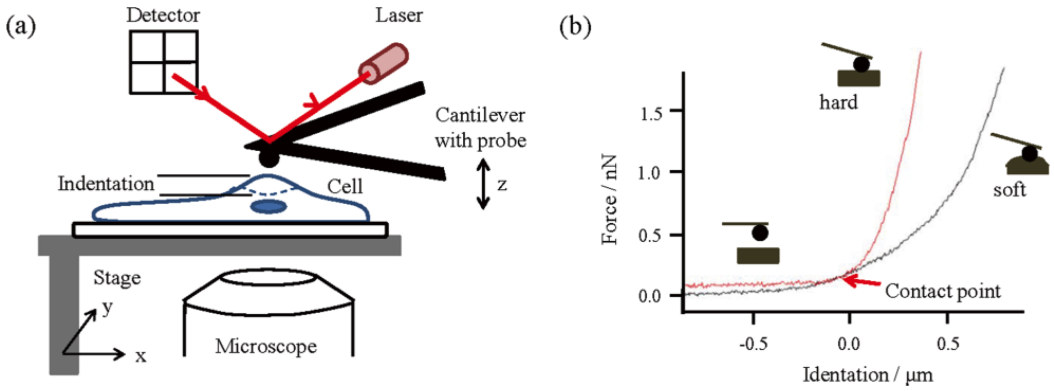

Fig. 1 (a) Principle of the AFM indentation measurement of the cell mechanical properties and (b) typical force-indentation curve.

can be calculated (Fig. 1). AFM has been extensively used to compare the stiffness of different cell types, especially for cancer and normal cells. It is an adequate instrument for revealing the relationship between the cytoskeleton structure and the cell mechanical properties, and has been proved to be one of the least invasive techniques for cell mechanical measurements.

Although lots of studies about the biomechanics have been done to discriminate cancer cells from normal cells, the mechanical difference between osteosarcoma and their normal counterparts still lacks investigation. Osteosarcoma is the most common bone cancer that is prevalent in children and young adults. Growing evidence suggests that osteosarcoma should be considered as a differentiation disease of osteoblast and MSC.[16] Understanding the different mechanical properties among these three types of cells should provide useful information for understanding the development of osteosarcoma. In this study, the morphological and mechanical properties of MSC, normal human osteoblast (NHOst) and osteosarcoma cells (MG-63) were compared using AFM indentation. The three types of cells represent the typical stem cells, somatic cells and cancer cells embedded in the osteosarcoma microenvironment. Also, the influence of the cytoskeleton structure on mechanotransduction was evaluated according to the expression of nuclear YAP/TAZ.

Experimental

Reagents and chemicals

Human bone marrow-derived MSC cells were purchased from Osiris Therapeutics, Inc. (Columbia, MA). The NHOst cells were purchased from Lonza Walkersville, Inc. (Walkersville, MD). MG-63 cells were acquired from Japanese Collection of Research Bioresources (JCRB) Cell Bank (Osaka, Japan). The growth media of MSC (MSC basal medium supplemented with 10% serum, 2% L-glutamine and 0.1% gentamicin sulfate amphotericin b) and NHOst cells (osteoblast basal medium supplemented with 10% serum, 0.1% ascorbic acid and 0.1% gentamicin sulfate amphotericin b) were purchased from Lonza Group Ltd. The growth medium of MG-63 cells (minimum essential medium eagle supplemented with 10% serum, 2 mM glutamine and 1% non essential amino acids) was purchased from Sigma-Aldrich (St. Louis, MO). Alexa Fluor-488 phalloidin and Alexa Fluor-488 labeled goat anti-mouse IgG antibody was purchased from Invitrogen (Carlsbad, CA). The 4′,6-diamidino-2-phenylindole (DAPI) was purchased from Vector Laboratories, Inc. (Burlingame, CA). Cytochalasin D (cyto D) was purchased from Sigma-Aldrich (St. Louis, MO). The mouse anti-YAP/TAZ primary antibody was purchased from Santa Cruz Biotechnology, Inc. (Dallas, TX).

Cell culture

The MSCs, NHOst and MG-63 cells were at first seeded at a low density (50 cells/cm^2) in 60 mm-diameter cell culture dishes to guarantee cell attachment in a single cell state. The cells were cultured using their respective growth medium for 24 h. Subsequently, the cells were merged in the HEPES medium to stabilize the pH value during the AFM measurement. To disrupt the actin structure, the growth medium containing 0.2 μg/ml cyto D was applied to cells 6 h post-seeding. After incubation for another 18 h, the cyto D containing medium was replaced with the HEPES medium, and the cyto D treated cells were used for an AFM measurement.

Atomic force microscopy

The cytoskeleton tension of living cells was evaluated using a commercially available MFP-3D-BIO AFM instrument (Asylum Research, Santa Barbara, CA) in a force mode. A silicon nitride cantilever (Novascan, Ames, IA) attached with a silica glass ball (diameter: 600 nm) as a probe was used for AFM nanoindentation. An optical microscope was used to visualize the cells and the position of the AFM tip. The spring constant of the cantilever was measured using the thermal tuning method.[17] The trigger force was set to 2 nN so as to avoid any damage to the cells. Each measurement was performed within a maximum of 1.5 h to minimize the death of cells during the experiment. The live/dead staining was performed to confirm the cell viability after a measurement. Force-volume height imaging (FVH) was firstly performed to characterize the morphological features of the three types of cells. The scan size was set to 20 pixel × 20 line with in 80 × 80 μm^2 area. Based on the acquired images, the force curves for stiffness measurement were collected at the highest region of cells with an indentation rate of 4 μm/s.

The Young's modulus of the cells was calculated using a Hertz's contact model.[18] For a spherical probe, the relationship between the loading force, F, and the indentation, δ, can be described by formula:

$$F(\delta) = \frac{4}{3} \cdot \sqrt{R} \cdot E_r \cdot \delta^{3/2}, \quad (1)$$

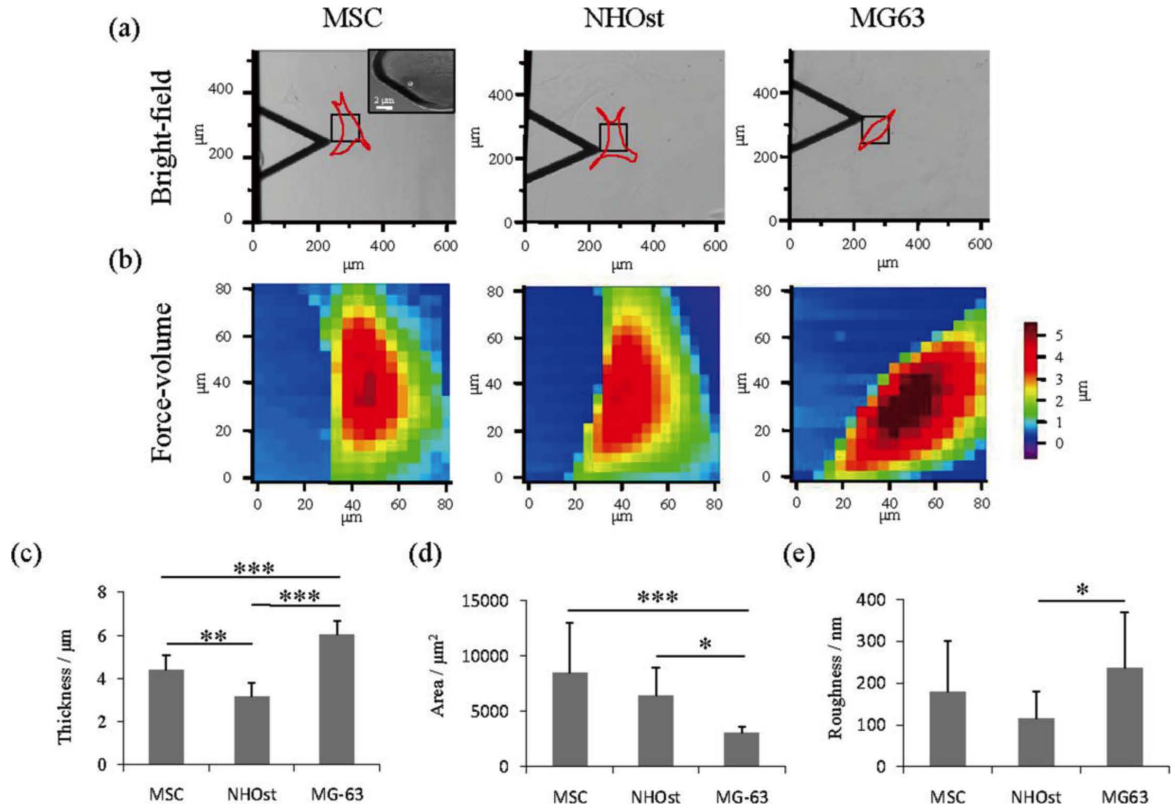

Fig. 2 Morphological features of osteosarcoma microenvironment cells. (a) Bright filed micrographs of cells during the AFM measurement. The red line represents the cell morphology observed by the microscope. (b) Force-volume height (FVH) map of MSC, NHOst and MG-63 cells measured within the black square in (a). (c) Thickness, (d) spreading area and (e) surface roughness of MSC, NHOst and MG-63 cells. The different morphologies indicated the intrinsic biophysical differences of these three types of cells. Above 30 individual cells were used for the morphological analysis of each cell type. All data represent the mean ± S.D. *, $p < 0.05$; **, $p < 0.01$; ***, $p < 0.001$.

where R is the radius of the tip and E_r is the reduced Young's modulus. In this study, the Young's modulus of the cells was calculated at a 200-nm indentation depth, which has been reported to be an abundant of actin network.[19] The reduced Young's modulus E_r correlates with the Young's modulus of sample E_s, and is given by:

$$\frac{1}{E_r} = \frac{1-{v_t}^2}{E_t} + \frac{1-{v_s}^2}{E_s}, \quad (2)$$

where v_t and v_s are the Poisson ratios of the tips and samples. When the Young's modulus of the tips is much greater than that of living cells, Eq. (2) can be simplified as follows:

$$E_r = \frac{E_s}{1-{v_s}^2}, \quad (3)$$

The Poisson ratio of a cell is assumed to be 0.5.[20]

The final stiffness of each cell type was determined by Gaussian fitting of the histogram created from the obtained Young's modulus. The center of the Gaussian fitting curve represents the average stiffness of the cell population; the half width at the half height represents the standard deviation (SD).[7]

F-actin staining

After incubation for 24 h, the cells were fixed with 4% cold paraformaldehyde. Then, the cells were permeabilized with 1% Triton X-100 for 2 min, and blocked with a 1% bovine serum albumin (BSA) solution for 30 min at room temperature. Actin filaments were stained by a treatment with Alexa Fluor-488 phalloidin for 20 min. DAPI was used to stain the nuclei. Fluorescence micrographs of the stained MSCs were captured using an Olympus BX51 microscope with a DP-70 CCD camera (Olympus, Tokyo, Japan).

YAP/TAZ staining

For YAP/TAZ staining, the fixed cells were permeated with 1% Triton X-100 and blocked with a 1% BSA solution for 30 min. Then, the samples were incubated with mouse anti-YAP/TAZ (1:100) at 4°C overnight, followed by PBS washing. Secondary antibody labeling was performed with Alexa Fluor-488 labeled goat anti-mouse IgG antibody (1:800) at room temperature for 1 h. Nuclei were stained with DAPI. The staining images were analyzed using a software ImageJ according to a previous report.[21]

Statistical analysis

Statistical analysis was performed using a one-way analysis of variance (ANOVA) with Tukey's post hoc test for multiple comparisons to confirm any significant differences among the samples. A value of $p < 0.05$ was considered to indicate a statistically significant difference.

Results and Discussion

Human MSC, NHOst and MG-63 cells were cultured in a growth medium at a low cell density to prevent cell-cell contact that may influence the cell mechanical properties.[22] The MSC and NHOst cells showed typical fibroblastic morphology with bipolar or multipolar elongated shapes. The MG-63 cells displayed a spindle-like morphology with a limited spreading area compared to MSC and NHOst cells (Fig. 2a). The typical force-height map of MSC, NHOst and MG-63 cells are shown in Fig. 2b. According to the force-height map, the highest part of cells was located near to the central region above the cell nucleus. In this study, the highest part of the cells was chosen to perform the measurement of cellular Young's modulus so as to avoid any influence of the substrate on the measurement.[23]

The thickness and spreading area of MSC, NHOst and MG-63 cells were different (Figs. 2c and 2d). MG-63 cells were the thickest cells among these three types with an average thickness of 6.04 ± 0.64 μm. This is in a good agreement with a previous study that showed that the cancer cells are significantly thicker than their normal counterparts.[24] MSC cells were significantly thicker than NHOst cells, and their thickness was 4.41 ± 0.65 and 3.17 ± 0.63 μm, respectively. The MSC and NHOst cells were significantly larger than MG-63 cells, while the size of MSC and NHOst cells was not significantly different. The spreading area of MSC and NHOst showed a big deviation, indicating the heterogeneity of the cells. The roughness of the cell membrane is an important cytological parameter that is involved in many biological processes, which is measured to predict the health state of cells.[25] A previous study reported that breast cancer cells are rougher than their normal counterparts, and that roughness increases with the increase of malignancy.[26] In this study, it was found that the MG-63 cells were significantly rougher than NHOst cells (Fig. 2e). It has been reported that the roughness of amniotic fluid-derived stem cells increases during osteogenic differentiation because of mineralization of the differentiated osteoblasts after an induction culture of 4 weeks.[27] However, according to our results, there was no significant difference of the surface roughness between MSC and NHOst cells, which may be due to the short cell culture time.

Histograms of the Young's modulus of MSC, NHOst and MG-63 cells are shown in Fig. 3. MSC and NHOst cells showed different histograms from that of MG-63 cells. The histogram of MSC and NHOst cells was very broad with a center peak value of 2.08 ± 1.13 and 2.42 ± 1.08 kPa, respectively. The Young's modulus of NHOst cells was significantly higher

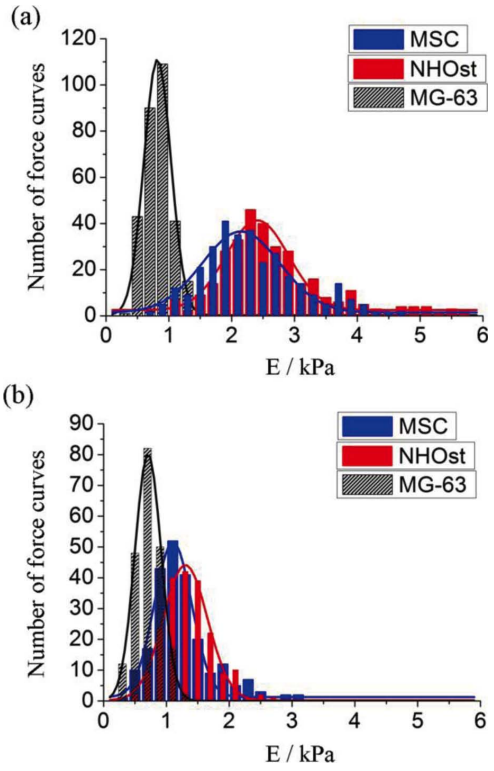

Fig. 3 Cell stiffness. The histograms of Young's modulus with Gaussian fittings obtained from (a) cyto D untreated and (b) cyto D treated MSC, NHOst and MG-63 cells. Above 200 force curves from more than 20 cells of each type were used for the calculation of Young's modulus.

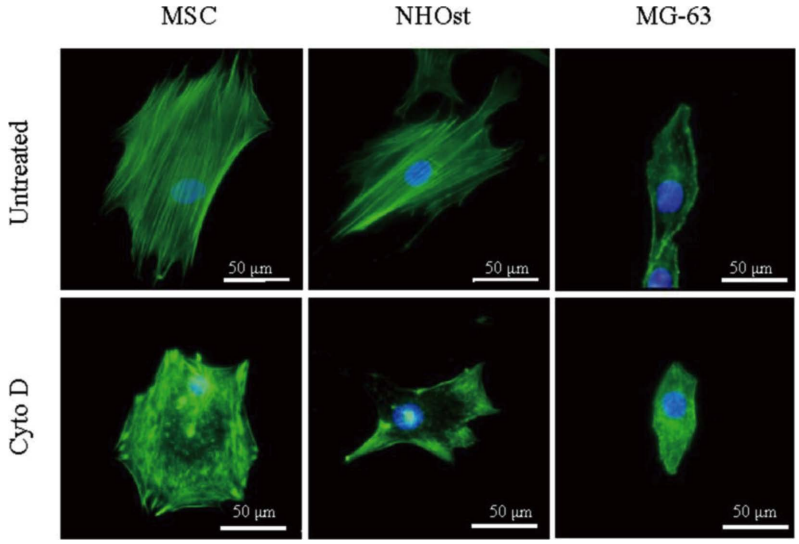

Fig. 4 Cell cytoskeleton assembly. The F-actin staining image of normal and cyto D treated MSC, NHOst and MG-63 cells.

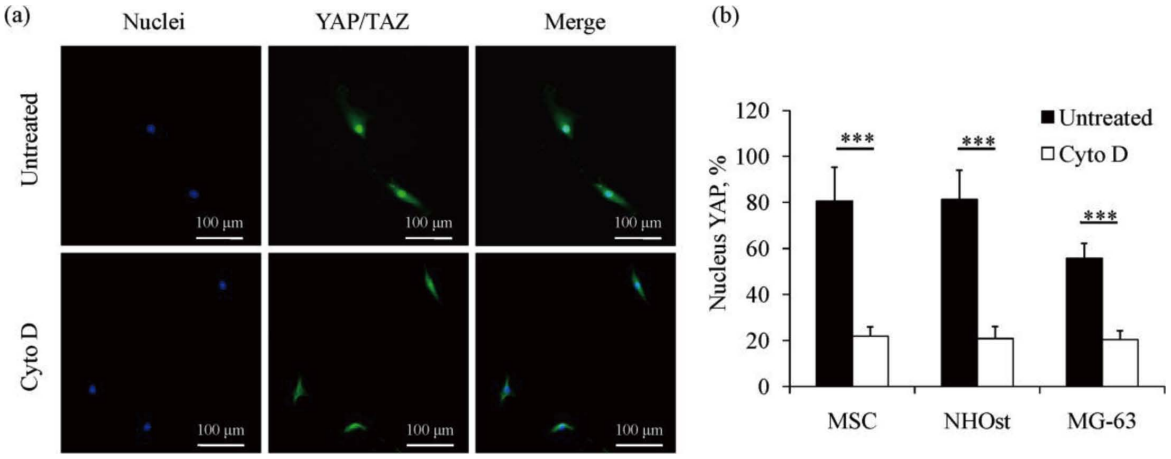

Fig. 5 Mechanotransduction of cells. (a) The typical YAP/TAZ staining images of MSC treated with and without cyto D. (b) Percentage of nuclear YAP/TAZ of cells treated with and without cyto D. ***, $p < 0.001$, $n = 3$.

($p \leq 0.001$) than that of MSC cells, indicating that mature osteoblasts were stiffer than their progenitor stem cells. Also, several studies have been reported that the Young's modulus of osteoblasts is higher than that of MSC, and that stiffness of MSC increases during osteogenic differentiation.[28,29] Both MSC and NHOst were significantly stiffer ($p \leq 0.001$) than MG-63 cells (0.82 ± 0.43 kPa). The results are in a good agreement with previous studies showing that cancer cells are softer than their normal counterparts.[5] In order to understand the relationship between the cytoskeleton structure and the cell stiffness, the three types of cells were treated with cyto D so as to disrupt the F-actin assembly. According to the indentation results, the treatment with cyto D caused a significant decrease ($p \leq 0.001$) of Young's modulus of all three types of cells, which is consistent with previous studies.[19,30] Especially for MSC and NHOst cells, the histogram exhibited a distinct distribution with a narrow and sharp peak compared to the cells without the cyto D treatment. The results indicated that the treatment of cyto D reduced the cell stiffness. The mechanical difference between MSC, NHOst and MG-63 cells may be used to discriminate the cancer cells from other cell types in their microenvironment.

The actin filaments are the major component of the cytoskeleton, which localizes beneath the cellular membrane and are supposed to play a crucial role in regulating cell mechanical properties.[6] The F-actin filament structure of MSC, NHOst and MG-63 cells was observed from fluorescence staining images (Fig. 4). Both MSC and NHOst showed abundant F-actin filaments according to the staining results. MSC had massive thin parallel actin filaments extending across the entire cell body. NHOst showed thick stress fibers constructed by actin filament bundles. The results confirmed that MSC change their cytoskeletal organization from thin to thick fibers during the osteogenic differentiation.[28,31] MG-63 cells formed actin fibers mainly at the cell periphery, and showed short actin filaments in the cell body region. Many other studies have also reported that the cancer cells, such as breast cancer cells,[6] bladder cancer cells[24] and thyroid cancer cells,[32] have a reduced organized actin filament structure compared to that of normal cells. After a treatment with cyto D, the actin filament organization in MSC and NHOst was disrupted, and the spindle-like MG-63 cells became elliptical.

YAP/TAZ has been reported be a sensor and mediator of mechanical cues.[1] And herein, the mechanotransduction of the three types of cells were evaluated based on their expression of nuclear YAP/TAZ. Typical YAP/TAZ staining images of MSC are shown in Fig. 5a. The percentage of nuclear YAP/TAZ of cells is shown in Fig. 5b. According to the results, MSC and NHOst had a higher percentage of nuclear YAP/TAZ compared to MG-63 cells, indicating that the high stiffness of MSC and NHOst facilitated a mechanotransduction of the cytoskeleton tension into nuclei. After the cyto D treatment, the percentage of nuclear YAP/TAZ significantly decreased, indicating that the disruption of the F-actin assembly would inhibit the mechanical force transduction.

Conclusions

In conclusion, the morphological and mechanical properties of the osteosarcoma microenvironment cells including MSC, NHOst and MG-63 cells were systemically compared using AFM. The MG-63 cells were thicker, smaller and rougher than the MSC amd NHOst cells. The MG-63 cells were softer than their normal counterparts due to their reduced organization of the cytoskeleton structure. A cyto D treatment disrupted the F-actin filament assembly, which resulted in a decrease of cell stiffness. The cell stiffness and the cytoskeleton structure affected the machanotransduction process. High stiffness and a well-organized assembly of the cytoskeleton promoted transduction of the cytoskeleton tension into nuclei, while low stiffness and a disruptted cytoskeleton structure inhibited the mechanotransduction. AFM should be a good tool to investigate the cell mechanical properties and should have a high potential of application for cancer diagnosis.

Acknowledgements

This work was supported by the World Premier International Research Center Initiative on Materials Nanoarchitectonics (WPI-MANA) and JSPS KAKENHI Grant Number 15J01781.

References

1. S. Dupont, L. Morsut, M. Aragona, E. Enzo, S. Giulitti,

M. Cordenonsi, F. Zanconato, J. Digabel, M. Forcato, S. Bicciato, N. Elvassore, and S. Piccolo, *Nature*, **2011**, *474*, 179.
2. B. Trappmann, J. E. Gautrot, J. T. Connelly, D. Strange, Y. Li, M. L. Oyen, M. Stuart, H. Boehm, B. Li, V. Vogel, J. P. Spatz, F. M. Watt, and W. Huck, *Nat. Mater.*, **2012**, *11*, 642.
3. L. B. Hazeltine, M. G. Badur, X. Lian, A. Das, W. Han, and S. P. Palecek, *Acta Biomater.*, **2014**, *10*, 604.
4. D. Li, J. Zhou, F. Chowdhury, J. Cheng, N. Wang, and F. Wang, *Regen. Med.*, **2011**, *6*, 229.
5. Q. S. Li, G. Lee, C. N. Ong, and C. T. Lim, *Biochem. Biophys. Res. Commun.*, **2008**, *374*, 609.
6. K. D. Costa, *Dis. Markers*, **2004**, *19*, 139.
7. M. Lekka, K. Pogoda, J. Gostek, O. Klymenko, S. Prauzner-Bechcicki, J. Wiltowska-Zuber, J. Jaczewska, J. Lekki, and Z. Stachura, *Micron*, **2012**, *43*, 1259.
8. J. Rother, H. Noding, I. Mey, and A. Janshoff, *Open Biol.*, **2014**, *4*, 140046.
9. N. Wang, J. P. Butler, and D. E. Ingber, *Science*, **1993**, *260*, 1124.
10. R. M. Hochmuth, *J. Biomech.*, **2000**, *33*, 15.
11. J. Guck, S. Schinkinger, B. Lincoln, F. Wottawah, S. Ebert, M. Romeyke, D. Lenz, H. M. Erickson, R. Ananthakrishnan, D. Mitchell, J. Kas, S. Ulvick, and C. Bilby, *Biophys. J.*, **2005**, *88*, 3689.
12. W. R. Legant, C. K. Choi, J. S. Miller, L. Shao, L. Gao, E. Betzig, and C. S. Chen, *Proc. Natl. Acad. Sci. U. S. A.*, **2013**, *110*, 881.
13. W. W. Hsiao, H. Liao, H. Lin, R. Ding, K. Huang, and C. Chang, *Anal. Sci.*, **2013**, *29*, 3.
14. W. W. Hsiao, H. Liao, H. Lin, Y. Lee, C. Fan, C. Liao, P. Lin, E. Hwu, and C. Chang, *Anal. Sci.*, **2013**, *29*, 885.
15. H. Liu, J. Wen, Y. Xiao, J. Liu, S. Hopyan, M. Radisic, C. A. Simmons, and Y. Sun, *ACS Nano*, **2014**, *8*, 3821.
16. N. Tang, W. Song, J. Luo, R. C. Haydon, and T. He, *Clin. Orthop. Relat. Res.*, **2008**, *466*, 2114.
17. X. Wang, X. Hu, J. Li, A. Russe, N. Kawazoe, Y. Yang, and G. Chen, *Biomater. Sci.*, **2016**, *4*, 970.
18. G. G. Adams and M. Nosonovsky, *Tribol. Int.*, **2000**, *33*, 431.
19. K. Pogoda, J. Jaczewska, J. Wiltowska-Zuber, O. Klymenko, K. Zuber, M. Fornal, and M. Lekka, *Eur. Biophys. J.*, **2012**, *41*, 79.
20. X. Wang, T. Nakamoto, I. Dulinska-Molak, N. Kawazoe, and G. Chen, *J. Mater. Chem. B*, **2016**, *4*, 37.
21. X. Wang, X. Hu, I. Dulinska-Molak, N. Kawazoe, Y. Yang, and G. Chen, *Sci. Rep.*, **2016**, *6*, 28708.
22. Q. Li, A. Kumar, E. Makhija, and G. V. Shivashankar, *Biomaterials*, **2014**, *35*, 961.
23. M. Lekka and P. Laidler, *Nat. Nanotechnol.*, **2009**, *4*, 72.
24. E. Canetta, A. Riches, E. Borger, S. Herrington, K. Dholakia, and A. K. Adya, *Acta Biomater.*, **2014**, *10*, 2043.
25. P. D. Antonio, M. Lasalvia, G. Perna, and V. Capozzi, *Biochim. Biophys. Acta*, **2012**, *1818*, 3141.
26. R. Kaul-Ghanekar, S. Singh, H. Mamgain, A. Jalota-Badhwar, K. M. Paknikar, and S. Chattopadhyay, *BMC Cancer*, **2009**, *9*, 350.
27. Q. Chen, P. Xiao, J. Chen, J. Cai, X. Cai, H. Ding, and Y. Pan, *Anal. Sci.*, **2010**, *26*, 1033.
28. G. Yourek, M. Hussain, and J. Mao, *ASAIO J.*, **2007**, *53*, 219.
29. E. M. Darling, M. Topel, S. Zauscher, T. P. Vail, and F. Guilak, *J. Biomech.*, **2008**, *41*, 454.
30. S. Barreto, C. H. Clausen, C. M. Perrault, D. Fletcher, and D. Lacroix, *Biomaterials*, **2013**, *34*, 6119.
31. J. P. Rodriguez, M. Gonzalez, S. Rios, and V. Cambiazo, *J. Cell Biochem.*, **2004**, *93*, 721.
32. M. Prabhune, G. Belge, A. Dotzauer, J. Bullerdiek, and M. Radmacher, *Micron*, **2012**, *43*, 1267.